IEEE Access
Multidisciplinary | Rapid Review | Open Access Journal

Received June 27, 2018, accepted July 31, 2018, date of publication August 7, 2018, date of current version August 28, 2018.

Digital Object Identifier 10.1109/ACCESS.2018.2864112

Digital Self-Interference Cancellation Based on Blind Source Separation and Spectral Efficiency Analysis for the Full-Duplex Communication Systems

HUA YANG[1], (Student Member, IEEE), HANG ZHANG[1], (Member, IEEE), JIANG ZHANG[2], AND LIU YANG[1], (Student Member, IEEE)

[1]College of Communication and Engineering, Army Engineering University of PLA, Nanjing 210007, China
[2]63rd Research Institute, National University of Defense Technology, Nanjing 210007, China

Corresponding author: Hang Zhang (hangzh_2002@163.com)

This work was supported by the Natural Science Foundation of China under Grant 61671475.

ABSTRACT In this paper, the fundamental problem for the full-duplex communication systems, i.e., self-interference cancellation (SIC), is investigated, and a novel digital-domain SIC method based on blind source separation is proposed. This method achieves SIC by separation and has two prominent characteristics that are: 1) it is a blind method, and no training sequence or time is needed and 2) it is unaffected by the nonlinear components of the self-interference signal. Meanwhile, the critical factors for spectral efficiency (SE) are fully analyzed herein. In the simulations, the performances of the proposed method, including SIC capacity, signal-to-interference-plus-noise ratio, SE, and SE gain, are comprehensively evaluated and compared with least-square-based SIC algorithms. These results show that the proposed algorithm can obtain considerable performances, even the best performance in some cases.

INDEX TERMS Full-duplex communication system, self-interference cancellation, blind source separation, oversampling, EASI, spectral efficiency.

I. INTRODUCTION

With the potential of doubling the spectral efficiency (SE) comparing to traditional half-duplex (HD) communication, full-duplex (FD) communication has received considerable interest or attention among researchers [1]–[5]. In addition, the increasingly intense contradiction between limited spectral resources and increasing spectral demands makes it more and more imminent to improve SE. In this situations, the FD communication is obviously a very appealing prospect. Therefore, it is considered as a candidate technology for 5G [6]–[8], i.e., the next generation mobile communication network.

The fundamental problem for FD communication system is self-interference (SI) caused by the operation of transmitting and receiving on same band simultaneously, i.e., local transmitted signal will couple back and leak to local receiver. Generally, SI signal may be nearly 60-100 dB stronger than the signal of interest (SoI) at receiver input, which would badly deteriorate the performance of FD communication system if without effective self-interference cancellation (SIC). Intuitively, SI signal can be easily cancelled by directly subtracting the transmitted signal from the received signal, as it comes from the local transmitter and is available to the receiver. However, the practical situation is that the effects of components within transceiver and coupling channel between transmitter and receiver should be completely taken into consideration to achieve a sufficient SIC [9]–[11]. These make SIC be a challenging issue.

SIC can be implemented mainly in three domains: propagation-domain, analog-circuit-domain, and digital-domain [3], [5], [12]–[14]. The propagation-domain SIC technologies include various antenna-based cancellation methods [15]–[17], duplexer [4], [5], [18], etc. These methods exploit special antenna deployments or structures to attenuate SI signal. The analog-circuit-domain SIC try to cancel SI signal in analog receive-chain circuitry by subtracting a predicted or regenerated SI signal from received signal before it is digitized [5], [10], [19], [20]. The predicted

SI signal can be generated by tapping the radio-frequency (RF) signal transmitted by local transmitter antenna, or by tapping the transmitted digital baseband signal and then converting to RF signal. The digital-domain SIC is carried out after analog-digital-converter (ADC), and many digital signal processing technologies [10], [21]–[24] can be utilized. In the digital-domain SIC, an equivalent discrete-time coupling channel is estimated to regenerate a digital SI signal. And then, the regenerated SI signal will be subtracted from the digital received signal. In general, any domain of SIC is inadequate to cancel SI signal down to an acceptable level for FD communication, they must be cascaded together to provide a joint SIC. In this paper, we mainly focus on the digital-domain SIC.

Traditional linear processing methods can only cancel the linear component of SI signal. However, it is not sufficient, as the residual nonlinear components of SI signal can still cause a serious interference to SoI due to its significantly higher power. The nonlinear components of SI signal are primarily caused by non-idealities of components within communication system. As analyzed in [11], the non-idealities mainly include nonlinear distortion of power amplifier (PA), impairment of I/Q mixer, phase noise of oscillators, quantization noise of ADC, etc. Many literatures have investigated the cancellation of nonlinear SI and greatly increase SIC capacity. As in [22], the I/Q imaging component caused by I/Q mixer is fully considered and a widely-linear SIC method is proposed. Overall considering nonlinear distortion of PA and I/Q mismatch of I/Q mixer, a complete digital cancellation method is developed in [25], this method further improves the SIC capacity.

Although, lots of methods have verified the good performance of SIC, the costs are relatively high. Some of them [22], [25], [36] need an extra calibration or training period to estimate SI channel, which really leads to a loss of SE, as no SoI is transmitted in this period. And, for some methods [27] that don't need calibration or training period, they simply treat SoI as an additive noise when estimating SI channel, which actually increases estimation variance and results in degradation of SIC capacity. Even more serious is that these methods may impair or attenuate SoI, because they only concentrate on the cancellation of SI signal rather than the recovery of SoI. That means more SIC not directly equal higher SE. The critical factors for SE will be fully analyzed in this paper.

Blind source separation (BSS) [28]–[32] is viewed as a powerful interference cancellation method, due to its ability of separating the mixture of signals that are non-Gaussian and mutually independent. That provides a completely new idea and horizon for SIC. As SI signal and SoI come from different transmitters and are non-Gaussian too, the preconditions for BSS are naturally satisfied, these provide a possibility for exploiting BSS method to perform the SIC for FD communication system. More attractive are that: a) BSS approach achieves SIC by separating rather than subtracting the regenerated SI signal, that can well maintain the integrality of SoI; b) it needs no extra training period, which avoids additional SE loss. As in [26], BSS is employed to SIC and achieves good performance. However, it needs an extra auxiliary receiver chain to offset the effect of nonlinear components of SI signal meanwhile satisfy the determined condition of BSS. As we know, smaller size [12] is also a pursuit for the device design of FD communication system. The extra auxiliary receiver chain is seemingly an expensive cost.

In this paper, a new BSS-based digital-domain SIC method is proposed for FD communication system with shared antenna. This method needs no extra auxiliary receiver chain, it just resorts to oversampling technology [33] to subtly transform the underdetermined mixing of signals into a determined mixing for facilitating the implementation of BSS. And, during separation, SI signal is equivalently treated as an independent source that makes this method be unaffected by the non-idealities of components within system. These guarantee predictable performances.

The rest of this paper is organized as follows. In section II, the frame structures of FD communication system along with the signal models are first introduced. Next, two least square (LS)-based contrast algorithms and the proposed algorithm are presented in section III. And the critical factors for SE are fully analyzed in section IV. Then, the performances for the three SIC algorithms including SIC capacity, signal-to-interference-plus-noise ratio (SINR), SE and SE gain are evaluated and compared in section V. Finally, the conclusions are made in section VI.

II. FULL-DUPLEX COMMUNICATION SYSTEM AND RECEIVED SIGNAL MODEL

In this section, the frame structures of FD communication system with shared antenna (i.e., the transmitter and receiver simultaneously use the same antenna via a 3-port circulator) are first described. And, the three domains SIC are overall employed in the system. Then, the effects of components with non-idealities on signal are elaborated. Finally, the SI signal and the received signal are accordingly modeled.

A. FULL-DUPLEX COMMUNICATION SYSTEM

As illustrated in Fig. 1, there is a simplified block diagram for a FD communication system with shared antenna, where the transmitter and receiver work on the same band simultaneously.

In the transmitter, local digital baseband signal Tb enters digital-analog-converter (DAC) and is converted into an analog signal. Then, the analog signal is up-converted to RF by I/Q mixer. The I/Q mismatch within the I/Q mixer may cause a generation of additional imaging component of the input signal. Meanwhile, there may come additional phase noise when the transmitter and receiver use different oscillators. After that, signal is amplified by PA. Due to the non-ideality of PA, there produces many nonlinear components, i.e., the high-order terms of its input signal. And then, the signal enters the circulator and couples with the antenna

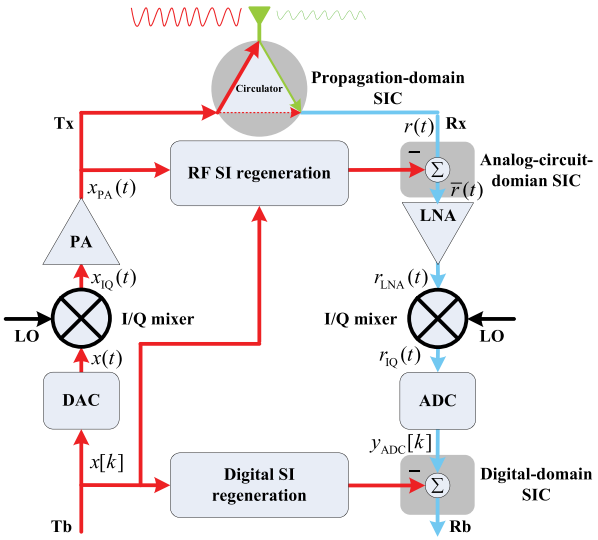

FIGURE 1. FD communication system with shared antenna.

for space propagation. As completed isolation is impossible, a leakage of the local transmitted signal through the circulator will enter the receiver chain and cause interference. The internal antenna reflection due to impedance mismatch between the isolator and antenna can also cause an interference to receiver. Another interference comes from the external reflections of transmitted signal from closely-located objects. All these form the final SI signal and enter the receiver chain.

In the receiver, the received signal (including the SI signal) continuously enters low-noise-amplifier (LNA) for power amplifying, I/Q mixer for down-converting to baseband, and analog-digital-converter (ADC) for converting to digital domain. In addition to additional noise caused by LNA, there are also some non-idealities in the receiver chain as in the transmitter chain. Certainly, some other components, e.g., shaping filter, low-pass-filter, band-pass-filter, and variable gain amplifier (VGA), are practically included in the FD communication system. And, they also are non-ideal, however, their negative effects can be negligible comparing to afore-mentioned those. For convenience of analysis, we omit these components in the diagram.

The three domains SIC are overall and necessarily employed in the FD communication system. As shown in Fig. 1, the isolation of circulator for transmitting and receiving serves as the propagation-domain SIC. By subtracting the regenerated RF SI signal, the analog-circuit-domain SIC is achieved. And the regeneration of RF SI signal can be implemented by tapping the local RF signal or by tapping the digital baseband signal and converting to RF. The digital-domain SIC is carried out by subtracting the regenerated digital SI signal from the received signal after ADC. Generally, the digital SI signal is generated according to an estimated SI channel. Final goal of the three domains SIC is to jointly cancel the SI signal down to a tolerable level, so as to make the SINR of SoI be adequate for subsequent processing, such as demodulating, decoding, etc.

B. RECEIVED SIGNAL MODEL

Before SIC, we should exactly know the concrete form of SI signal. However, the components of communication system generally are non-ideal that makes the SI signal be different from what we intuitively considered. In the following, we will detail the SI signal form according to the characteristics of components.

Assume that the analog baseband transmitted signal is denoted by $x(t)$. And, it is the digital-to-analog conversion of digital baseband transmitted signal $x[k]$ (i.e., Tb, see Fig. 1), which is accurately known to the local receiver. In consideration of the practically existed I/Q mismatch, the output signal of I/Q mixer can be written as

$$x_{\mathrm{IQ}}(t) = g_1 x(t) + g_2 x^*(t) \tag{1}$$

where g_1 and g_2 represent the responses to the signal component and imaging component of $x(t)$, respectively. And superscript * denotes the conjugate operator. The quality of I/Q mixer can be measured by image rejection ratio (IRR), which is defined as

$$\mathrm{IRR} = 20\log_{10}\left(\frac{|g_1|}{|g_2|}\right) \tag{2}$$

After I/Q mixer, signal $x_{\mathrm{IQ}}(t)$ is amplified by PA. The non-ideality of PA makes its output signal be a polynomial function of its input signal. The model of PA can be characterized by the Hammerstein nonlinearity [27]. Then, the output signal of PA can be expressed as

$$x_{\mathrm{PA}}(t) = \left(\sum_{p=1,p\in odd}^{P} a_p x_{\mathrm{IQ}}(t)\left|x_{\mathrm{IQ}}(t)\right|^{p-1}\right) * f(t) \tag{3}$$

where a_1 is the gain of linear component, $a_{p,p\neq 1}$ is the gain of nonlinear component, and P is the nonlinear order. In addition, $f(t)$ denotes the memory function of PA, and $*$ represents the convolution operator. In fact, the settings $P = 3$ and $f(t) = \delta(t)$ are widely used and are sufficient. In that case, the output signal of PA can be simplified as

$$x_{\mathrm{PA}}(t) = a_1 x_{\mathrm{IQ}}(t) + a_3 x_{\mathrm{IQ}}(t)\left|x_{\mathrm{IQ}}(t)\right|^2 \tag{4}$$

And then, the amplified signal enters circulator and couples with antenna for space propagation.

As operating on the same band simultaneously, local transmitted signal would couple back to local receiver chain and cause SI. Then, the totally received signal in the receiver can be expressed as

$$r(t) = x_{\mathrm{PA}}(t) * h_1(t) + s(t) * h_2(t) + n(t) \tag{5}$$

where $x_{\mathrm{PA}}(t) * h_1(t)$ is the SI term, $s(t)$ denotes the SoI, and $n(t)$ is the thermal noise. And, $h_1(t)$ and $h_2(t)$ represent the channels of SI and SoI, respectively. Before LNA, the analog-circuit-domain SIC is performed to suppress the SI signal, and $x_{\mathrm{PA}}(t)$ is served as the original SI signal to regenerate the

practical RF SI signal that contains the impact of channel, then the received signal can be expressed as

$$\begin{aligned}\bar{r}(t) &= r(t) - x_{\mathrm{PA}}(t) * \hat{h}(t) \\ &= x_{\mathrm{PA}}(t) * \left(h_1(t) - \hat{h}(t)\right) + s(t) * h_2(t) + n(t) \\ &= x_{\mathrm{PA}}(t) * \tilde{h}_1(t) + s(t) * h_2(t) + n(t) \end{aligned} \tag{6}$$

where $\hat{h}(t)$ denotes the predicted analog SI signal channel, $x_{\mathrm{PA}}(t) * \hat{h}(t)$ is served as the regenerated RF SI signal, and $\tilde{h}_1(t)$ represents the residual analog SI signal channel. Certainly, the RF SI signal can also be regenerated according to the digital baseband transmitted signal $x[k]$. For the sake of concision, we don't detail it here.

Next, $\bar{r}(t)$ is amplified by the LNA, and the output signal can be written as

$$r_{\mathrm{LNA}}(t) = g_{\mathrm{LNA}}\bar{r}(t) + n_{\mathrm{LNA}}(t) \tag{7}$$

where g_{LNA} is the gain of LNA, and $n_{\mathrm{LNA}}(t)$ is the noise introduced by LNA.

Similarly, I/Q mixer in receiver has I/Q mismatch, its output can be expressed as

$$r_{\mathrm{IQ}}(t) = g_3 r_{\mathrm{LNA}}(t) + g_4 (r_{\mathrm{LNA}}(t))^* \tag{8}$$

where g_3 and g_4 denote the responses of the signal component and imaging component of $r_{\mathrm{LNA}}(t)$, respectively.

Finally, $r_{\mathrm{IQ}}(t)$ is digitized by ADC for subsequent processing. And, a VGA is necessary to adjust the signal power to match the voltage range of ADC. Thus, the digital received signal can be written as

$$\begin{aligned} y_{\mathrm{ADC}}[k] &= y_{\mathrm{ADC}}(kT_s) \\ &= g_{\mathrm{VGA}} r_{\mathrm{IQ}}(kT_s) + n_{\mathrm{ADC}}(kT_s) \\ &= g_{\mathrm{VGA}} r_{\mathrm{IQ}}[k] + n_{\mathrm{ADC}}[k] \end{aligned} \tag{9}$$

where g_{VGA} is the gain of VGA, $n_{\mathrm{ADC}}[k]$ is the quantization noise caused by ADC, and T_s is the symbol period. In general, the imaging component caused by I/Q mixer in receiver can be neglected due to adequate IRR when emphasizing on the SIC. Thus, the final digital received signal can be modeled as

$$\begin{aligned} y_{\mathrm{ADC}}[k] &= g_{\mathrm{VGA}} r_{\mathrm{IQ}}[k] + n_{\mathrm{ADC}}[k] \\ &= g_{total} x_{\mathrm{PA}}[k] * \tilde{h}_1[k] + g_{total} s[k] * h_2[k] + \tilde{n}[k] \end{aligned} \tag{10}$$

where

$$g_{total} = g_{\mathrm{VGA}} g_3 g_{\mathrm{LNA}} \tag{11}$$

$$\tilde{n}[k] = g_{total} n[k] + g_{\mathrm{VGA}} g_3 n_{\mathrm{LNA}}[k] + n_{\mathrm{ADC}}[k] \tag{12}$$

From (10), we can know that the residual SI signal in digital-domain comes from the item $g_{total} x_{\mathrm{PA}}[k] * \tilde{h}_1[k]$.

III. DIGITAL-DOMAIN SIC ALGORITHMS

In this section, we will focus on how to cancel the residual SI signal in digital-domain for FD communication systems. A new BSS-based digital-domain SIC method is developed herein. And, by contrast, two LS-based digital-domain SIC algorithms are introduced first.

A. LS-BASED DIGITAL-DOMAIN SIC ALGORITHMS

The key to digital-domain SIC is how to accurately model and regenerate the SI signal. More accurate regeneration means more cancellation.

Traditional LS-based digital-domain SIC method directly utilizes the digital baseband transmitted signal, i.e., $x[k]$, as reference/training samples to estimate the SI channel, as it is available to the receiver. Then, the estimated SI channel is employed to regenerate the SI signal, which will finally be subtracted from the received signal. We will elaborate in the following.

The digital received signal model expressed in (10) can be reformed as (subscript $_{\mathrm{ADC}}$ is omitted)

$$\begin{aligned} y[k] &= \sum_{l=0}^{L} \left(g_{total} x_{\mathrm{PA}}[k-l]\tilde{h}_1[l] + g_{total} s[k-l] h_2[l]\right) + \tilde{n}[k] \\ &= \sum_{l=0}^{L} (x[k-l]h_{\mathrm{SI}}[l] + s[k-l]h_{\mathrm{SoI}}[l]) + d[k] + \tilde{n}[k] \\ &= \sum_{l=0}^{L} (x[k-l]h_{\mathrm{SI}}[l] + s[k-l]h_{\mathrm{SoI}}[l]) + \tilde{d}[k] \end{aligned} \tag{13}$$

where $L+1$ equals the channel time-spreading length, $h_{\mathrm{SI}}[l]$ is the channel impulse response (CIR) corresponding to the linear component of SI signal, $s[k]$ represents the digital SoI, $h_{\mathrm{SoI}}[l]$ is the CIR of digital SoI, $d[k]$ contains all the residual imaging and nonlinear components of SI signal, and $\tilde{d}[k] = d[k] + \tilde{n}[k]$. Usually, SoI is considered as additional noise when estimating the SI channel. And, accordingly, the estimation accuracy is low. Thus, we assume that a length of N additional training samples from far transmitter are provided. Then, in addition to $h_{\mathrm{SI}}[l]$, $h_{\mathrm{SoI}}[l]$ is estimated too.

Transforming (13) into a matrix form and gathering N observations, we have

$$\begin{aligned} \mathbf{y} &= \mathbf{X}\mathbf{h}_{\mathrm{SI}} + \mathbf{S}\mathbf{h}_{\mathrm{SoI}} + \tilde{\mathbf{d}} \\ &= [\mathbf{X}, \mathbf{S}]\left[(\mathbf{h}_{\mathrm{SI}})^T, (\mathbf{h}_{\mathrm{SoI}})^T\right]^T + \tilde{\mathbf{d}} \\ &= \tilde{\mathbf{X}}\mathbf{h} + \tilde{\mathbf{d}} \end{aligned} \tag{14}$$

where $\mathbf{y} = [y[k], y[k-1], \ldots, y[k-N+1]]^T$ denotes the received signal vector, superscript ^{T} is the transpose operator, $\tilde{\mathbf{X}} = [\mathbf{X}, \mathbf{S}]$, $\mathbf{h} = \left[(\mathbf{h}_{\mathrm{SI}})^T, (\mathbf{h}_{\mathrm{SoI}})^T\right]^T$, $\mathbf{h}_{\mathrm{SI}} = [h_{\mathrm{SI}}(0), \ldots, h_{\mathrm{SI}}(L)]^T$, $\mathbf{h}_{\mathrm{SoI}} = [h_{\mathrm{SoI}}(0), \ldots, h_{\mathrm{SoI}}(L)]^T$, and $\tilde{\mathbf{d}} = \left[\tilde{d}[k], \tilde{d}[k-1], \ldots, \tilde{d}[k-N+1]\right]^T$. And,

$$\mathbf{X} = \begin{bmatrix} x[k] & x[k-1] & \ldots & x[k-L] \\ x[k-1] & x[k-2] & \ldots & x[k-L-1] \\ \vdots & \vdots & \ddots & \vdots \\ x[k-N+1] & x[k-N] & \ldots & x[k-L-N+1] \end{bmatrix} \tag{15}$$

$\mathbf{S}$ has the same structure as $\mathbf{X}$. According to the LS principle, channel vector $\mathbf{h}$ can be estimated as

$$\hat{\mathbf{h}} = (\tilde{\mathbf{X}}^H \tilde{\mathbf{X}})^{-1} \tilde{\mathbf{X}}^H \mathbf{y} \tag{16}$$

where superscript ^{H} denotes the conjugate transpose operator. In that way, the estimations of $\mathbf{h}_{\mathrm{SI}}$ and $\mathbf{h}_{\mathrm{SoI}}$ are both obtained, i.e., $\hat{\mathbf{h}}_{\mathrm{SI}}$ and $\hat{\mathbf{h}}_{\mathrm{SoI}}$. Then, these channel estimations are used to regenerate the SI signal. In addition, the delayed components of SoI also are treated as interferences for the purpose of deconvolution. Thus, digital-domain SIC can be implemented as

$$\begin{aligned}\hat{s}[k] &= y[k] - \mathbf{x}^T\hat{\mathbf{h}}_{\mathrm{SI}} - \tilde{\mathbf{s}}^T\tilde{\hat{\mathbf{h}}}_{\mathrm{SoI}} \\ &= h_{\mathrm{SoI}}[0]s[k] + \sum_{l=0}^{L} x[k-l]\left(h_{\mathrm{SI}}[l] - \hat{h}_{\mathrm{SI}}[l]\right) \\ &\quad + \sum_{l=1}^{L} s[k-l]\left(h_{\mathrm{SoI}}[l] - \hat{h}_{\mathrm{SoI}}[l]\right) + \tilde{d}[k] \end{aligned} \tag{17}$$

where $\hat{s}[k]$ denotes the recovered SoI, $\mathbf{x}^T\hat{\mathbf{h}}_{\mathrm{SI}}$ represents the regenerated SI signal, $\mathbf{x}^T = [x[k], \ldots, x[k-L]]$, $\tilde{\mathbf{s}}^T\tilde{\hat{\mathbf{h}}}_{\mathrm{SoI}}$ is the delay interference, $\tilde{\mathbf{s}}^T = [s[k-1], \ldots, s[k-L]]$, and $\tilde{\hat{\mathbf{h}}}_{\mathrm{SoI}} = \left[\hat{h}_{\mathrm{SoI}}[1], \hat{h}_{\mathrm{SoI}}[2], \ldots, \hat{h}_{\mathrm{SoI}}[L]\right]^T$. In a compact form, (17) can be rewritten as

$$\hat{s}[k] = h_{\mathrm{SoI}}[0]s[k] + e[k] \tag{18}$$

where $e[k]$ contains all the other residual interferences and noise, it impacts the quality of SoI and indicates the SIC capacity.

As described above, traditional LS-based SIC algorithm only concentrates on the cancellation of the linear component of SI signal. However, it is inadequate as the residual imaging and nonlinear components still have strong power and can badly deteriorate the quality of SoI. In [25], a new LS-based joint cancellation algorithm that can handle the joint effects of I/Q mismatch and PA nonlinearity is proposed. The prominent characteristic is the reference signal (traditional reference signal is only the digital baseband transmitted signal $x[k]$) that is used to estimate the CIR. The reference signal is formed as

$$\psi\left(x[k], q, p\right) = (x[k])^q\left(x^*[k]\right)^{p-q} \tag{19}$$

where $\psi(\cdot)$ is the basis function, $q = 1, 2, \ldots, p$ and $p = 1, 3, \ldots, P$. In that case, the digital received signal model can be reformed as

$$\begin{aligned} y[k] = &\sum_{p=1, p\in odd}^{P}\sum_{q=0}^{p}\sum_{l=0}^{L}(x[k-l])^q\left(x^*[k-l]\right)^{p-q}h_{\mathrm{SI}}^{q,p-q}[l] \\ &+ \sum_{l=0}^{L} s[k-l]h_{\mathrm{SoI}}[l] + \tilde{d}[k] \end{aligned} \tag{20}$$

where $h_{\mathrm{SI}}^{q,p-q}[l]$ is the channel impulse response corresponding to $(x[k-l])^q(x^*[k-l])^{p-q}$. Taking the same operations as in (14), we have

$$\begin{aligned} y[k] &= \boldsymbol{\psi}\tilde{\mathbf{h}}_{\mathrm{SI}} + \mathbf{S}\mathbf{h}_{\mathrm{SoI}} + \tilde{\mathbf{d}} \\ &= [\boldsymbol{\psi}, \mathbf{S}]\left[\left(\tilde{\mathbf{h}}_{\mathrm{SI}}\right)^T, \left(\mathbf{h}_{\mathrm{SoI}}\right)^T\right]^T + \tilde{\mathbf{d}} \\ &= \tilde{\boldsymbol{\psi}}\tilde{\mathbf{h}} + \tilde{\mathbf{d}} \end{aligned} \tag{21}$$

where $\tilde{\boldsymbol{\psi}} = [\boldsymbol{\psi}, \mathbf{S}]$, $\tilde{\mathbf{h}} = \left[\left(\tilde{\mathbf{h}}_{\mathrm{SI}}\right)^T, \left(\mathbf{h}_{\mathrm{SoI}}\right)^T\right]^T$, $\boldsymbol{\psi}$ is a horizontal concatenation of the matrices, $\boldsymbol{\psi}_{q,p}$, as shown at the bottom of this page, and $\tilde{\mathbf{h}}_{\mathrm{SI}}$ is a vertical concatenation of the vectors

$$\mathbf{h}_{\mathrm{SI}}^{q,p-q} = \left[h_{\mathrm{SI}}^{q,p-q}[0], h_{\mathrm{SI}}^{q,p-q}[1], \ldots, h_{\mathrm{SI}}^{q,p-q}[L]\right]^T \tag{23}$$

with $q = 1, 2, \ldots, p$ and $p = 1, 3, \ldots, P$. Thus, the estimation of $\tilde{\mathbf{h}}$ is calculated as

$$\hat{\tilde{\mathbf{h}}} = (\tilde{\boldsymbol{\psi}}^H\tilde{\boldsymbol{\psi}})^{-1}\tilde{\boldsymbol{\psi}}^H\mathbf{y} \tag{24}$$

And the subsequent digital-domain SIC can be performed as in (17).

Because the reference signal components are more integrated, they can better model the SI signal. Then, this new LS-based SIC algorithm greatly outperforms the traditional LS-based SIC algorithm. For distinction, we name this new LS-based SIC algorithm as JLS.

B. BSS-BASED DIGITAL-DOMAIN SIC ALGORITHM

As SI signal and SoI come from different transmitters, they are mutually independent naturally. Also, they are non-Gaussian. These provide a possibility for exploiting BSS method to perform the SIC. More important is that this method is unaffected by the components of SI signal, as the SI signal can be integrally treated as a source signal, which will lead to better SIC. In addition, no extra training samples are needed for this method, which means that SE can be improved, or in other words, extra SE loss can be avoided.

As BSS method is unaffected by the components of signal, for the convenience of derivations, we define the SI symbol as $x_{\mathrm{SI}}[k]$, the SoI symbol as $x_{\mathrm{SoI}}[k]$, the generalized CIR corresponding to SI signal as $c_{\mathrm{SI}}[l]$, and the generalized CIR corresponding to SoI as $c_{\mathrm{SoI}}[l]$. The received signal can be modeled as (the noise item is omitted)

$$\begin{aligned} y[k] &= \sum_{l=0}^{L}\left(x_{\mathrm{SI}}[k-l]c_{\mathrm{SI}}[l] + x_{\mathrm{SoI}}[k-l]c_{\mathrm{SoI}}[l]\right) \\ &= \sum_{l=0}^{L}\mathbf{c}^T[l]\widehat{\mathbf{x}}[k-l] \\ &= \sum_{l=0}^{L}\mathbf{c}^T[k-l]\widehat{\mathbf{x}}[l] \end{aligned} \tag{25}$$

$$\boldsymbol{\psi}_{q,p} = \begin{bmatrix} \psi\left(x[k], q, p\right) & \cdots & \psi\left(x[k-L], q, p\right) \\ \vdots & \vdots & \ddots \\ \psi\left(x[k-N+1], q, p\right) & \cdots & \psi\left(x[k-L-N+1], q, p\right) \end{bmatrix} \tag{22}$$

where $\mathbf{c}^T[k-l] = [c_{\mathrm{SI}}[k-l], c_{\mathrm{SoI}}[k-l]]$, and $\widehat{\mathbf{x}}[l] = [x_{\mathrm{SI}}[l], x_{\mathrm{SoI}}[l]]^T$.

SIC can be implemented by separation according to the independence between SI signal and SoI. However, the mixing model, as described in (25), is an undetermined mixing that is hard to separate. Then, the oversampling method [33] is adopted to transform the undetermined mixing into a determined mixing as it can provide additional information about the mixing procedure. Oversampling the received signal by the times of $2(L+1)$, we have

$$\begin{aligned} y(kT_s + \frac{m}{M}T_s) &= \sum_{l=0}^{L} \mathbf{c}^T \left((k-l)T_s + \frac{m}{M}T_s\right)\widehat{\mathbf{x}}[l] \\ &= \sum_{l=0}^{L} \mathbf{c}^T \left(lT_s + \frac{m}{M}T_s\right)\widehat{\mathbf{x}}[k-l] \end{aligned} \tag{26}$$

where $m \in [0, 1, \ldots, M-1]$, and $M = 2(L+1)$. Reforming (26) into a matrix form, we have

$$\begin{aligned} \tilde{\mathbf{y}}[k] &= \begin{bmatrix} \mathbf{c}_0^T[0] & \mathbf{c}_0^T[1] & \cdots & \mathbf{c}_0^T[L] \\ \mathbf{c}_1^T[0] & \mathbf{c}_1^T[1] & \cdots & \mathbf{c}_1^T[L] \\ \vdots & \vdots & \ddots & \vdots \\ \mathbf{c}_{2L+1}^T[0] & \mathbf{c}_{2L+1}^T[1] & \cdots & \mathbf{c}_{2L+1}^T[L] \end{bmatrix} \tilde{\widehat{\mathbf{x}}}[k] \\ &= \mathbf{C}\tilde{\widehat{\mathbf{x}}}[k] \end{aligned} \tag{27}$$

where $\tilde{\mathbf{y}}[k] = \left[y(kT_s), y(kT_s + \frac{1}{M}T_s), \ldots, y(kT_s + \frac{M-1}{M}T_s)\right]^T$, $\tilde{\mathbf{y}}[k] \in \mathbb{C}^{2(L+1)\times 1}$, $\mathbf{c}_m^T[l] = \mathbf{c}^T(lT_s + \frac{m}{M}T_s)$, $\mathbf{C} \in \mathbb{C}^{2(L+1)\times 2(L+1)}$ denotes the extended mixing matrix, $\tilde{\widehat{\mathbf{x}}}[k] = \left[\widehat{\mathbf{x}}[k]^T, \ldots, \widehat{\mathbf{x}}[k-L]^T\right]^T$, and $\tilde{\widehat{\mathbf{x}}}[k] \in \mathbb{C}^{2(L+1)\times 1}$. The elements of $\tilde{\widehat{\mathbf{x}}}[k]$ can be treated as mutually independent sources, as the SI symbols and SoI symbols are independent identically distributed sequences respectively. Meanwhile, the CIRs (i.e., $c_{\mathrm{SI}}[l]$ and $c_{\mathrm{SoI}}[l]$) usually are not identical that makes the extended mixing matrix $\mathbf{C}$ be nonsingular or full rank [33]. In that way, the undetermined mixing is transformed into a determined mixing that will facilitate the implementation of BSS.

BSS procedure can estimate a separating matrix $\mathbf{W} \in \mathbb{C}^{2(L+1)\times 2(L+1)}$ that makes the global matrix $\mathbf{G} \in \mathbb{C}^{2(L+1)\times 2(L+1)}$, defined as $\mathbf{G} = \mathbf{WC}$, be a generalized permutation matrix (i.e., there is only one non-zero element in each row and column). Then, the SIC can be implemented as

$$\mathbf{z}[k] = \mathbf{W}\tilde{\mathbf{y}}[k] = \mathbf{WC}\tilde{\widehat{\mathbf{x}}}[k] = \mathbf{G}\tilde{\widehat{\mathbf{x}}}[k] \tag{28}$$

where $\mathbf{z}[k] \in \mathbb{C}^{2(L+1)\times 1}$ denotes the separated signal vector. As $\mathbf{G}$ is a generalized permutation matrix, the entries of $\mathbf{z}[k]$ are effective estimations of the entries of $\tilde{\widehat{\mathbf{x}}}[k]$. There is up to an ambiguity of order and scaling (phase and amplitude) between the two signal vectors. In other words, the superposition of the SI signal and the SoI is separated, which is equivalent to the cancellation of SI signal. Surely, an extraction of the SoI from the separated signals is necessary. Due to it is not the focus of this paper, we no longer expatiate on it.

In this paper, the classical EASI [33], [34] algorithm is utilized to perform the digital-domain SIC. However, some modifications, detailed in Appendix, are made to fit the complex characteristic of signals and to accelerate the convergence speed. The iterative procedure of separating matrix $\mathbf{W}$ is formed as (see Appendix for details)

$$\mathbf{W}[k+1] = \mathbf{W}[k] - \mu[\boldsymbol{\varphi}(\mathbf{z}[k])\,\mathbf{z}^H[k] - \frac{1}{2}\mathbf{I} + \mathbf{T}[k]]\mathbf{W}[k] \tag{29}$$

IV. SE ANALYSIS

Dose FD communication double SE? The practical situation is that the achievable SE gain of FD communication always less than 2, as SIC cannot be perfect. In this section, we will analyze the factors that impact the SE.

The achievable SE of HD communication can be formulated as

$$\begin{aligned} SE_{\mathrm{HD}} &= \log_2(1 + \frac{P_{\mathrm{SoI}}}{P_{\mathrm{RDI}} + P_n}) \\ &= \log_2(1 + SINR_{\mathrm{HD}})[\mathrm{bps/Hz}] \end{aligned} \tag{30}$$

where $P_{\mathrm{SoI}} = |h_{\mathrm{SoI}}[0]|^2\,\mathrm{E}\left\{|s[k]|^2\right\}$ denotes the power of SoI, P_{RDI} represents the power of residual delay components due to imperfect deconvolution, P_n is the power of noise, and $SINR_{\mathrm{HD}} = \frac{P_{\mathrm{SoI}}}{P_{\mathrm{RDI}}+P_n}$ is defined as the SINR in HD communication mode.

By contrast, the achievable SE of FD communication after LS-based SIC can be expressed as (unit is omitted)

$$\begin{aligned} SE_{\mathrm{FD,LS}} &= 2\log_2(1 + \frac{P_{\mathrm{SoI}}}{P_{\mathrm{RSI}} + P_{\mathrm{RDI}} + P_n}) \\ &= 2\log_2(1 + SINR_{\mathrm{FD,LS}}) \end{aligned} \tag{31}$$

where P_{RSI} denotes the power of residual SI signal, and $SINR_{\mathrm{FD,LS}} = \frac{P_{\mathrm{SoI}}}{P_{\mathrm{RSI}}+P_{\mathrm{RDI}}+P_n}$ is defined as the SINR in FD communication mode. The pre-log factor 2 is benefited from that FD communication equivalently has two-way rate as transmitting and receiving on the same band simultaneously.

From (30) and (31), we can observe that the residual power of SI signal makes $SE_{\mathrm{FD,LS}}$ always be less than $2SE_{\mathrm{HD}}$. In general, more SIC means higher SE. However, sometimes it not always hold. When the regeneration of SI signal is greater than the practical SI signal in power, achievable SE will actually decrease, because SI is over-cancelled, which would lead to a loss of SoI power. In that case, the achievable SE can be reformed as

$$SE_{\mathrm{FD,LS}} = 2\log_2(1 + \frac{P_{\mathrm{SoI}} - P_{\mathrm{OCSI}}}{P_{\mathrm{RDI}} + P_n}) \tag{32}$$

where P_{OCSI} denotes the over-cancelled power of SI signal.

And, the achievable SE when employing BSS-based SIC can be formulated as

$$\begin{aligned} SE_{\mathrm{FD,BSS}} &= 2\log_2(1 + \frac{\tilde{P}_{\mathrm{SoI}}}{P_{\mathrm{RI}} + \tilde{P}_n}) \\ &= 2\log_2(1 + SINR_{\mathrm{FD,BSS}}) \end{aligned} \tag{33}$$

where $\tilde{P}_{\mathrm{SoI}} = |g_{\mathrm{BSS}}|^2\,\mathrm{E}\left\{|x_{\mathrm{SoI}}[k]|^2\right\}$ denotes the power of the recovered SoI, g_{BSS} is the power gain when using BSS-based

SIC algorithm, P_{RI} represents the power of all residual interference, $\tilde{P}_n$ is the noise power and $SINR_{\mathrm{FD,BSS}} = \frac{\tilde{P}_{\mathrm{SoI}}}{P_{\mathrm{RI}}+\tilde{P}_n}$ is defined as the SINR with BSS-based SIC.

Generally, LS-based SIC methods need separate calibration or training time to estimate SI channel, which means no SoI is transmitted in this period and then leads to a loss of SE. Assume that $\rho \in [0, 1)$ is the proportion of training time to transmitting time. Then, the final achievable SE can be expressed as (subscripts are omitted for simplicity)

$$SE = 2(1-\rho)\log_2(1+SINR) \tag{34}$$

It is a general formula for achievable SE. And $\rho = 0$ means no training time is needed, e.g., BSS-based SIC.

V. EXPERIMENTAL SIMULATIONS

In this section, the two LS-based and the BSS-based algorithms, discussed in section III, are used to perform the digital-domain SIC. In order to determine the performances of BSS-based approach in comparison to the two LS-based algorithms, four performance metrics are evaluated, including SIC capacity, SINR, SE, and SE gain.

In the simulations, the modulation schemes of local and far transmitters both are 4QAM and the non-idealities of I/Q mixer and PA are all considered. In addition, nonlinear rejection ratio (NRR) is defined to assess the effect of nonlinear distortion of PA, that is

$$\mathrm{NRR} = 20\log_{10}(\frac{|a_1|}{|a_3|}) \tag{35}$$

For LS-based algorithms, the training samples length is set to $N = 10000$, and the BSS-based approach uses the same length of signals for iterations. The depth factor w of BSS-based algorithm is set to 2. Assume that the time-spreading length $L+1$ is 3. And channel coefficients are randomly generated complex variables with absolute value belonging to (0, 1).

A. SIC CAPACITY

The SIC capacity, defined as the difference of the output signal-to-self-interference ratio (SIR) and input SIR, is first evaluated. As shown in Fig. 2, the SIC capacities of JLS algorithm significantly outperform the other two algorithms under different self-interference-to-signal ratio (ISR), IRR, and NRR conditions. In addition, the SIC capacities of JLS and BSS algorithms gradually improve with ISR increasing and are nearly unaffected by IRR and NRR. By contrast, the SIC capacity of LS algorithm decreases around 10 dB, when the values of IRR and NRR drop to 20 dB both from 30 dB both. It demonstrates the weaker cancellation ability of LS algorithm for the nonlinear components of SI signal. Meanwhile its performances are insensitive to ISR. Moreover, the SIC capacities of BSS algorithm perform better than LS algorithm when IRR = 20 dB and NRR = 20 dB with all ISR conditions. However, for the conditions of IRR = 30 dB and IRR = 30 dB, it not hold until ISR greater than 20 dB.

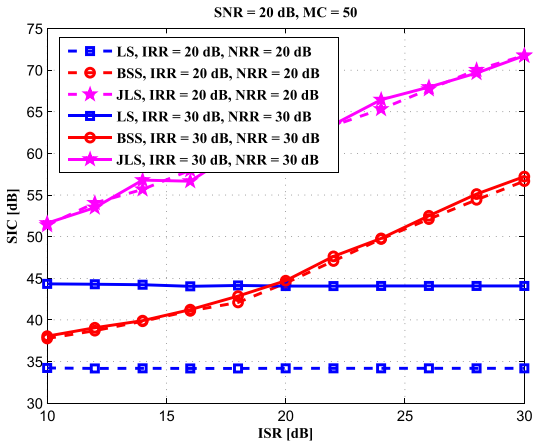

FIGURE 2. SIC capacities vs. ISR for the three SIC algorithms under different IRR and NRR conditions. The signal-to-noise ratio (SNR) equals 20 dB, and Monte Carlo (MC) simulation times are 50.

The SIC capacities with respect to SNR under different IRR and NRR conditions are shown in Fig. 3. JLS algorithm also has the best performance in all conditions. And BSS algorithm always outperforms LS algorithm when IRR = 20 dB and NRR = 20 dB. In the conditions IRR = 30 dB and IRR = 30 dB, when SNR greater than 14 dB BSS algorithm is better than LS algorithm.

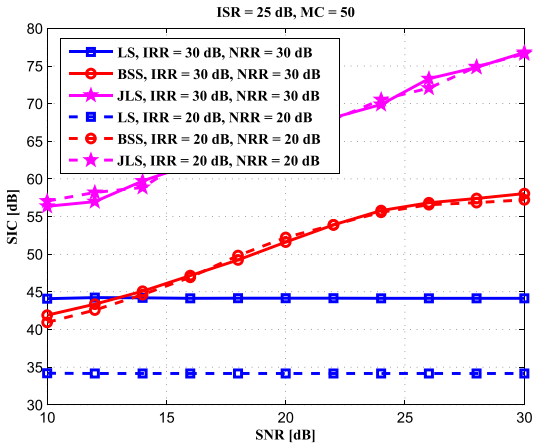

FIGURE 3. SIC capacities vs. SNR for the three SIC algorithms under different IRR and NRR conditions.

B. SE

As SINR is the critical factor for SE, it is assessed before SE. As shown in Fig. 4, the SINRs of JLS and BSS algorithms also are robust to IRR and NRR, but LS algorithm is not. However, the superiority of JLS algorithm is reduced, as over-SIC may occur that has a negative effect on SINR. In addition, the advantages of BSS to LS also decline. The reason is that BSS may gather additional noise during separation, which weakens the SINR.

SEs for the three SIC algorithms are shown in Fig. 5. All the three algorithms improve SE contrasted to HD when IRR = 30 dB and IRR = 30 dB. However, when conditions come

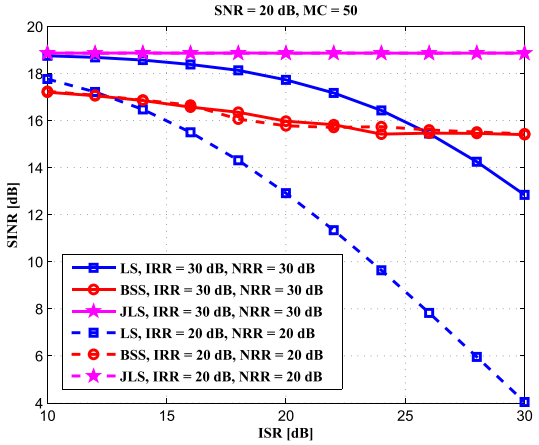

FIGURE 4. SINRs vs. ISR for the three SIC algorithms.

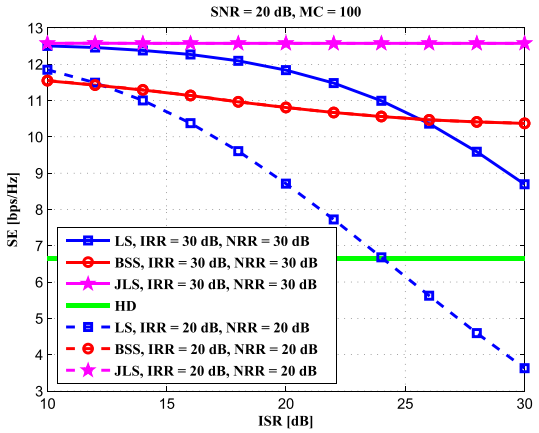

FIGURE 5. SEs vs. ISR for the three SIC algorithms.

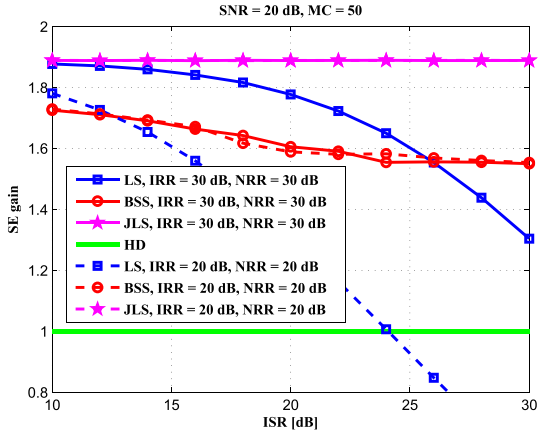

FIGURE 6. SE gains vs. ISR for the three SIC algorithms.

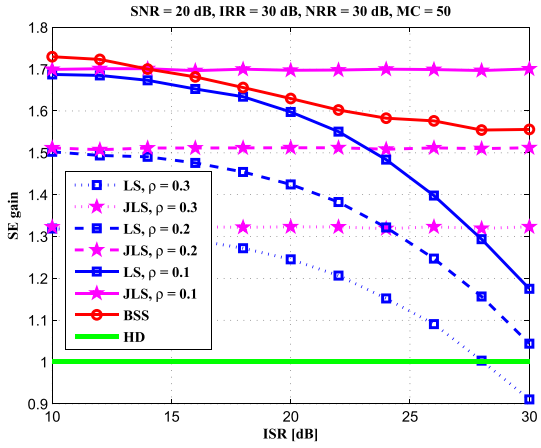

FIGURE 7. SE gains vs. ISR for the three SIC algorithms with different ρ.

to IRR $=$ 20 dB and NRR $=$ 20 dB, the SE of LS even less than HD when ISR greater than 24 dB.

In Fig. 6, accurate SE gains for the three SIC algorithm are illustrated. JLS algorithm can obtain nearly 1.9 times SE gain in all conditions. And, for BSS algorithm, its SE gains gradually decrease from about 1.75 to 1.55 times along with ISR increasing. In addition, for LS algorithm, SE gains are lost when ISR greater than 24 dB with IRR $=$ 20 dB and NRR $=$ 20 dB. In another IRR and NRR conditions, its SE gains drop fast from nearly 1.9 to 1.3 times when ISR increasing.

Considering that training time plays an important role in SE, we theoretically test the SE gains with different ρ. As no training time is needed for BSS algorithm, the value of ρ is 1. From Fig. 7, we can know that the superiority of JLS to BSS is completely vanished when $\rho \geq 0.2$. The reason is that the overhead of training time for LS-based SIC algorithms consequentially leads to SE loss. However, BSS-based SIC algorithm effectively avoids this overhead, thus the SE is improved essentially.

From the simulations, we can conclude that:

1) The performances of JLS and BSS algorithms are robust to IRR and NRR, i.e., they are unaffected by the imaging and nonlinear components of SI signal. However, LS algorithm do not have this characteristic;
2) More SIC do not always mean higher SINR or SE, as over-SIC may occur and noise level may increase during processing;
3) The overhead of training time would lead to SE loss, which makes BSS-based SIC algorithm can outperform the JLS algorithm in some cases.

VI. CONCLUSIONS

In this paper, we investigate the SI problem encountering in the FD communication systems. Two LS-based and a new BSS-based digital-domain SIC algorithms are introduced. The new BSS-based SIC algorithm can achieve the SIC by separation only according to the independence between the SI signal and SoI. In addition, this method needs no training samples and is unaffected by the components of SI signal. The critical factors for SE is also completely analyzed herein. Four performance metrics are evaluated for the three SIC algorithms in the simulations. Those simulation results confirm that the proposed SIC algorithm can obtain considerable

performances, and in some cases it even has the best performance.

APPENDIX

The objective function of EASI is formulated as

$$\Phi(\mathbf{W}) = -\sum_{i=1}^{N_s} \mathrm{E}\left\{\log\left(f_z(z_i)\right)\right\} - \log\left|\det(\mathbf{W})\right| \tag{36}$$

where $\mathrm{E}\{\cdot\}$ denotes the expectation operator, $f_z(z_i)$ represents the probability density function (PDF) of the separated signal z_i, z_i is the i th component of $\mathbf{z}$, $\mathbf{z} \in \mathbb{C}^{N_s \times 1}$ is the separated signal vector, N_s is the number of sources, i.e., $N_s = 2(L+1)$, and $\det(\cdot)$ is the determinant function. As baseband communication signal has complex characteristic, the iterative direction of $\mathbf{W}$ accordingly becomes the conjugate natural gradient direction of the objective function $\Phi(\mathbf{W})$, that is

$$\Delta\mathbf{W} \propto \frac{\partial\Phi(\mathbf{W})}{\partial\mathbf{W}^*}\mathbf{W}^H\mathbf{W} \tag{37}$$

where

$$\frac{\partial\Phi(\mathbf{W})}{\partial\mathbf{W}^*} = -\sum_{i=1}^{N_s}\mathrm{E}\left\{\frac{\partial\log\left(f_z(z_i)\right)}{\partial {z_i}^*}\frac{\partial {z_i}^*}{\partial\mathbf{W}^*}\right\} - \frac{1}{\left|\det(\mathbf{W})\right|}\frac{\partial\left|\det(\mathbf{W})\right|}{\partial\mathbf{W}^*} \tag{38}$$

with

$$\mathbf{z} = \mathbf{W}\tilde{\mathbf{y}} \tag{39}$$

$$\frac{\partial {z_i}^*}{\partial\mathbf{W}^*} = \frac{\partial(\mathbf{w}_i\tilde{\mathbf{y}})^*}{\partial\mathbf{W}^*} = \left[\mathbf{0}_{N_s\times(i-1)}, \tilde{\mathbf{y}}^*, \mathbf{0}_{N_s\times(N_s-i)}\right]^T \tag{40}$$

$$\begin{aligned}\frac{1}{\left|\det(\mathbf{W})\right|}\frac{\partial\left|\det(\mathbf{W})\right|}{\partial\mathbf{W}^*} &= \frac{1}{\left|\det(\mathbf{W})\right|}\frac{\partial[(\det(\mathbf{W})^*)(\det(\mathbf{W}))]^{\frac{1}{2}}}{\partial\mathbf{W}^*} \\ &= \frac{1}{2}(\mathbf{W}^H)^{-1}\end{aligned} \tag{41}$$

where $\mathbf{w}_i$ is the i th row of $\mathbf{W}$, and $\mathbf{0}$ is the zero matrix. Then, the iterative procedure of $\mathbf{W}$ can be formulated as

$$\begin{aligned}\mathbf{W}[k+1] &= \mathbf{W}[k] - \mu\frac{\partial\Phi(\mathbf{W})}{\partial\mathbf{W}^*[k]}\mathbf{W}^H[k]\mathbf{W}[k] \\ &= \mathbf{W}[k] - \mu[\boldsymbol{\varphi}\left(\mathbf{z}[k]\right)\mathbf{z}^H[k] - \frac{1}{2}\mathbf{I}]\mathbf{W}[k]\end{aligned} \tag{42}$$

where $\mu \in (0, 1]$ denotes the step size, k represents the time index, $\boldsymbol{\varphi}(\mathbf{z}) = [\varphi_z(z_1), \varphi_z(z_2), \ldots, \varphi_z(z_{N_s})]^T$, $\varphi_z(z_i) = -\frac{\partial\log(f_z(z_i))}{\partial {z_i}^*}$ is termed as the nonlinear kernel function (NKF), and $\mathbf{I} \in \mathbb{R}^{N_s\times N_s}$ is the identity matrix. Usually, a correction term is added for stability. Then, the final iterative formula of $\mathbf{W}$ is obtained, that is

$$\mathbf{W}[k+1] = \mathbf{W}[k] - \mu[\boldsymbol{\varphi}\left(\mathbf{z}[k]\right)\mathbf{z}^H[k] - \frac{1}{2}\mathbf{I} + \mathbf{T}[k]]\mathbf{W}[k] \tag{43}$$

where $\mathbf{T}[k] = \mathbf{z}[k]\mathbf{z}^H[k] - \mathbf{z}[k]\boldsymbol{\varphi}^H\left(\mathbf{z}[k]\right)$ is the correction term.

For the choice of NKF, we exploit the constellation distribution of signals to build the probability model, as in [35], which means a more accurate NKF and then a faster convergence speed. The local transmitter and far transmitter generally use the same modulation scheme. Although there are some non-idealities of the components within the system, these hardly effect the probability distribution of signals. The PDF of signals can be modeled as

$$f_z(z_i) = \sum_{m=1}^{M} w\left(1 - \tanh^2(w\left|z_i - A_m\right|)\right) \tag{44}$$

where M is redefined as the modulation order of signals here, w denotes the depth factor, and $\{A_m\}_{m=1,2,\ldots,M}$ represents the signal constellation. Then, the NKF can be calculated as

$$\begin{aligned}\varphi_z(z_i) &= -\frac{\partial\log\left(f_z(z_i)\right)}{\partial {z_i}^*} \\ &= -\sum_{m=1}^{M}\frac{w^2 v_{i,m}\tanh(w\left|v_{i,m}\right|)\left(1-\tanh^2(w\left|v_{i,m}\right|)\right)}{\left|v_{i,m}\right| f_z(z_i)}\end{aligned} \tag{45}$$

where $v_{i,m} = z_i - A_m$.

ACKNOWLEDGMENT

The authors would like to thank the anonymous reviewers and the editors for helping to improve this work.

REFERENCES

[1] M. Duarte and A. Sabharwal, "Full-duplex wireless communications using off-the-shelf radios: Feasibility and first results," in *Proc. Conf. Rec. 44th Asilomar IEEE Signals, Syst. Comput. (ASILOMAR)*, Nov. 2010, pp. 1558–1562.

[2] M. Duarte, C. Dick, and A. Sabharwal, "Experiment-driven characterization of full-duplex wireless systems," *IEEE Trans. Wireless Commun.*, vol. 11, no. 12, pp. 4296–4307, Dec. 2012.

[3] J. I. Choi, M. Jain, K. Srinivasan, P. Levis, and S. Katti, "Achieving single channel, full duplex wireless communication," in *Proc. 16th Annu. Int. Conf. Mobile Comput. Netw.*, 2010, pp. 1–12.

[4] A. Sabharwal, P. Schniter, D. Guo, D. W. Bliss, S. Rangarajan, and R. Wichman, "In-band full-duplex wireless: Challenges and opportunities," *IEEE J. Sel. Areas Commun.*, vol. 32, no. 9, pp. 1637–1652, Sep. 2014.

[5] D. Bharadia, E. McMilin, and S. Katti, "Full duplex radios," *ACM SIGCOMM Comput. Commun. Rev.*, vol. 43, no. 4, pp. 375–386, 2013.

[6] Z. Zhang, X. Chai, K. Long, A. V. Vasilakos, and L. Hanzo, "Full duplex techniques for 5G networks: Self-interference cancellation, protocol design, and relay selection," *IEEE Commun. Mag.*, vol. 53, no. 5, pp. 128–137, May 2015.

[7] N. H. Mahmood, G. Berardinelli, F. M. L. Tavares, and P. E. Mogensen, "On the potential of full duplex communication in 5G small cell networks," in *Proc. IEEE 81st IEEE Veh. Technol. Conf. (VTC Spring)*, May 2015, pp. 1–5.

[8] S. Hong *et al.*, "Applications of self-interference cancellation in 5G and beyond," *IEEE Commun. Mag.*, vol. 52, no. 2, pp. 114–121, Feb. 2014.

[9] E. Ahmed, A. M. Eltawil, and A. Sabharwal, "Rate gain region and design tradeoffs for full-duplex wireless communications," *IEEE Trans. Wireless Commun.*, vol. 12, no. 7, pp. 3556–3565, Jul. 2013.

[10] T. Riihonen and R. Wichman, "Analog and digital self-interference cancellation in full-duplex MIMO-OFDM transceivers with limited resolution in A/D conversion," in *Proc. Conf. Rec. 46th Asilomar IEEE Signals, Syst. Comput. (ASILOMAR)*, Nov. 2012, pp. 45–49.

[11] D. W. Bliss, T. M. Hancock, and P. Schniter, "Hardware phenomenological effects on cochannel full-duplex MIMO relay performance," in *Proc. Conf. Rec. 46th IEEE Signals, Syst. Comput. (ASILOMAR)*, Nov. 2012, pp. 34–39.

[12] G. Liu, F. R. Yu, H. Ji, V. C. M. Leung, and X. Li, "In-band full-duplex relaying: A survey, research issues and challenges," *IEEE Commun. Surveys Tuts.*, vol. 17, no. 2, pp. 500–524, 2nd Quart., 2015.

[13] M. Heino, D. Korpi, and T. Huusari, "Recent advances in antenna design and interference cancellation algorithms for in-band full duplex relays," *IEEE Commun. Mag.*, vol. 53, no. 5, pp. 91–101, May 2015.

[14] A. Masmoudi and T. Le-Ngoc, "Channel estimation and self-interference cancelation in full-duplex communication systems," *IEEE Trans. Veh. Technol.*, vol. 66, no. 1, pp. 321–334, Jan. 2017.

[15] E. Everett, A. Sahai, and A. Sabharwal, "Passive self-interference suppression for full-duplex infrastructure nodes," *IEEE Trans. Wireless Commun.*, vol. 13, no. 2, pp. 680–694, Feb. 2014.

[16] K. Yang, H. Cui, L. Song, and Y. Li, "Efficient full-duplex relaying with joint antenna-relay selection and self-interference suppression," *IEEE Trans. Wireless Commun.*, vol. 14, no. 7, pp. 3991–4005, Jul. 2015.

[17] B. van Liempd *et al.*, "RF self-interference cancellation for full-duplex," in *Proc. 9th Int. Conf. IEEE Cogn. Radio Oriented Wireless Netw. Commun. (CROWNCOM)*, Jun. 2014, pp. 526–531.

[18] M. E. Knox, "Single antenna full duplex communications using a common carrier," in *Proc. IEEE 13th Annu. Wireless Microw. Technol. Conf. (WAMICON)*, Apr. 2012, pp. 1–6.

[19] K. Chang, S.-A. Kim, and J. U. H. Sik, "Method and apparatus for canceling self-interference," U.S. Patent 0 218 769 A1, Jul. 28, 2016.

[20] A. Sahai, G. Patel, and A. Sabharwal. (2011). "Pushing the limits of full-duplex: Design and real-time implementation." [Online]. Available: https://arxiv.org/abs/1107.0607

[21] E. Ahmed and A. M. Eltawil, "All-digital self-interference cancellation technique for full-duplex systems," *IEEE Trans. Wireless Commun.*, vol. 14, no. 7, pp. 3519–3532, Jul. 2015.

[22] D. Korpi, L. Anttila, V. Syrjälä, and M. Valkama, "Widely linear digital self-interference cancellation in direct-conversion full-duplex transceiver," *IEEE J. Sel. Areas Commun.*, vol. 32, no. 9, pp. 1674–1687, Sep. 2014.

[23] E. Ahmed, A. M. Eltawil, and A. Sabharwal, "Self-interference cancellation with nonlinear distortion suppression for full-duplex systems," in *Proc. Asilomar Conf. IEEE Signals, Syst. Comput.*, Nov. 2013, pp. 1199–1203.

[24] L. Anttila, D. Korpi, V. Syrjala, and M. Valkama, "Cancellation of power amplifier induced nonlinear self-interference in full-duplex transceivers," in *Proc. Asilomar Conf. IEEE Signals, Syst. Comput.*, Nov. 2013, pp. 1193–1198.

[25] L. Anttila, D. Korpi, E. Antonio-Rodríguez, R. Wichman, and M. Valkama, "Modeling and efficient cancellation of nonlinear self-interference in MIMO full-duplex transceivers," in *Proc. IEEE Globecom Workshops (GC Wkshps)*, Dec. 2014, pp. 777–783.

[26] J. Li, H. Zhang, and M. Fan, "Digital self-interference cancellation based on independent component analysis for co-time co-frequency full-duplex communication systems," *IEEE Access*, vol. 5, pp. 10222–10231, 2017.

[27] T. Le-Ngoc and A. Masmoudi, "Self-interference-cancellation in full-duplex systems," in *Full-Duplex Wireless Communications Systems*. Cham, Switzerland: Springer, 2017, pp. 13–25.

[28] G. Huang and L. Yang, "A radar anti-jamming technology based on blind source separation," in *Proc. 7th Int. Conf. Signal Process. (ICSP)*, vol. 3, Aug. 2004, pp. 2021–2024.

[29] B. Lin, B.-N. Zhang, and D.-S. Guo, "Blind source separation in noisy environment and applications in satellite communication anti-jamming," in *Proc. Asia–Pacific Conf. IEEE Comput. Intell. Ind. Appl. (PACIIA)*, vol. 2, Nov. 2009, pp. 96–99.

[30] V. Zarzoso and A. K. Nandi, "Blind source separation," in *Blind Estimation Using Higher-Order Statistics*. Boston, MA, USA: Springer, 1999, pp. 167–252.

[31] A. Hyvarinen, J. Karhunen, and E. Oja, "Independent component analysis," in *Natural Image Statistics*. Hoboken, NJ, USA: Wiley, 2004.

[32] *Handbook of Blind Source Separation: Independent Component Analysis and Applications*. New York, NY, USA: Academic, 2010.

[33] Y. Zhang and S. A. Kassam, "Blind separation and equalization using fractional sampling of digital communications signals," *Signal Process.*, vol. 81, no. 12, pp. 2591–2608, 2001.

[34] J.-F. Cardoso and B. H. Laheld, "Equivariant adaptive source separation," *IEEE Trans. Signal Process.*, vol. 44, no. 12, pp. 3017–3030, Dec. 1996.

[35] K. Torkkola, "Blind signal separation in communications: Making use of known signal distributions," in *Proc. IEEE Digit. Signal Process. Workshop*, Aug. 1998, pp. 1–4.

[36] K. Dani, A. Lauri, and V. Mikko, "Impact of received signal on self-interference channel estimation and achievable rates in in-band full-duplex transceivers," in *Proc. 48th Asilomar Conf. Signals, Syst. Comput.*, Nov. 2014, pp. 975–982.

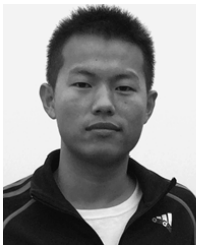

HUA YANG (S'15) received the B.S. degree in information warfare technology from the Beijing Institute of Technology, Beijing, China, in 2013, and the M.S. degree in information and communications engineering from the PLA University of Science and Technology, Nanjing, China, in 2016. He is currently pursuing the Ph.D. degree in information and communications engineering with the Army Engineering University of PLA.

His current research interests include signal processing, blind source separation, and interference cancellation.

HANG ZHANG (M'12) received the B.S. degree from the PLA University of Science and Technology, Nanjing, China, in 1984, and the M.S. degree from Southeast University, Nanjing, in 1989.

She is currently a Professor and also a Ph.D. Supervisor with the Army Engineering University of PLA. Her research interests include wireless communication, satellite communication, and signal processing.

JIANG ZHANG received the B.S. degree in communication engineering from the Taiyuan University of Technology, Taiyuan, China, in 2006, and the M.S. and Ph.D. degrees in information and communications engineering from the PLA University of Science and Technology, Nanjing, China, in 2009 and 2013, respectively.

He is currently an Engineer with the 63rd Research Institute, National University of Defense Technology. His research interests include anti-jamming, signal processing, and blind source separation.

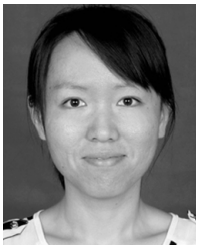

LIU YANG (S'15) received the B.S. and M.S. degrees in communication engineering and information and communications engineering from the PLA University of Science and Technology, Nanjing, China, in 2012 and 2015, respectively. She is currently pursuing the Ph.D. degree in information and communications engineering with the Army Engineering University of PLA.

Her research interests include communications anti-jamming, signal processing, and blind source separation.